THE EFFECT OF SILICA NANOPARTICLES ON CORROSION OF STEEL BY MOLTEN CARBONATE EUTECTICS

A Thesis

by

ASHWIN PADMANABAN IYER

Submitted to the Office of Graduate Studies of
Texas A&M University
in partial fulfillment of the requirements for the degree of

MASTER OF SCIENCE

May 2011

Major Subject: Mechanical Engineering

THE EFFECT OF SILICA NANOPARTICLES ON CORROSION OF STEEL BY MOLTEN CARBONATE EUTECTICS

A Thesis

by

ASHWIN PADMANABAN IYER

Submitted to the Office of Graduate Studies of
Texas A&M University
in partial fulfillment of the requirements for the degree of

MASTER OF SCIENCE

Approved by:

Co-Chairs of Committee,	Thomas Lalk
	Michael Schuller
Committee Member,	Ted Hartwig
Head of Department,	Dennis O'Neal

May 2011

Major Subject: Mechanical Engineering

ABSTRACT

The Effect of Silica Nanoparticles on Corrosion of Steel by Molten Carbonate Eutectics.

(May 2011)

Ashwin Padmanaban Iyer, B.E., Visvesvaraya Technological University India

Co-Chairs of Advisory Committee: Dr. Thomas Lalk
Dr. Michael Schuller

The effect of silica nanoparticles on corrosion of steel by molten carbonate eutectic (42.7% Li_2CO_3, K_2CO_3) was investigated. The experimental design was based on static coupon immersion methodology where a coupon (material under study, in this case a rectangular stainless steel specimen of SS304 with dimensions approximately 5X20X.6mm and weight .5gm) is exposed to a static corroding environment for predetermined periods of time. The testing times were 2, 4 and 6 weeks. The temperature during testing was maintained at a constant 520C. The instantaneous corrosion rates were determined by normalizing the mass loss with respect to time and area. The mass loss was determined by descaling the corroded steel coupons using concentrated hydrochloric acid. The instantaneous corrosion rates obtained from all three times showed a reduction in corrosion of steel by molten carbonate eutectics when doped with silica 1% by weight in comparison to the molten base carbonate eutectics.

The results showed that doping the carbonate eutectic with silica nanoparticles (1% by weight) reduced the corrosion of steel by half in comparison to the corrosion without doping.

DEDICATION

For my parents and my family without whose support this would not have been possible.

ACKNOWLEDGEMENTS

I would like to thank all the committee members for their guidance and support. I would like to thank all the students who worked in this project with me. I would also thank my parents for providing me an opportunity.

TABLE OF CONTENTS

Page

Page

LIST OF FIGURES

Page

LIST OF TABLES

Page

1. INTRODUCTION

The current energy demands have necessitated the need for renewable energy sources. Solar energy can be a very good source of renewable energy. Concentrated solar power (CSP) are systems that use lenses or mirrors to concentrate a large area of sunlight onto a small area. This concentration of sunlight produces significant amounts of heat energy which is trapped and channeled through a collector fluid. This heat energy from the collector fluid is then transferred to a storage system which stores the heat. But storing the thermal energy has been found to be difficult (1). However, storing energy is the only way for CSP's to handle load requirements during the night.

Thermal energy storage (TES) materials are those materials that store energy by virtue of latent or sensible heat or both. These materials have high energy densities and hence are used to store thermal energy. TES material is typically stored in steel containers. However, one characteristic of these TES materials is that they are corrosive. Not only is the chemical characteristic of the TES very corrosive, but the high temperatures associated with heat storage makes the situation worse. The typical temperatures in a CSP are in the range of 500-600C.

This thesis follows the style of ASME Journal of Solar Energy Engineering.

But these limitations cannot be a roadblock to solar energy development, especially in a world plagued with energy crisis. One way to improve the efficiency of a solar energy system is by enhancing the thermophysical properties of TES which brings about a reduction in $/KWh. In the current context, this enhancement of thermophysical properties was done using silica nanoparticles. But a useful byproduct of this enhancement of thermophysical properties of base carbonate eutectics by silica nanoparticles may have a positive effect on reducing corrosion. The motive behind this hypothesis is that Sugema et al (2) have shown that silica mitigates corrosion. As such improving or modifying the existing TES materials to further improve the heat storage capability may further strengthen the use of clean and green solar energy. Doing so will reduce the operating cost which will eventually translate in reduction of cost of electricity to the final consumer.

As such, I investigated the effect of modified/improved TES materials on corrosion. Here the term modification implies addition of silica nanoparticles to improve the thermophysical properties of the TES. If the process of modifying/improving TES materials for improving thermophysical properties also has a positive effect in reduction of corrosion, it will further boost the justification of such TES material modification techniques and hence the use of solar energy. The next two sections gives a brief overview of a TES and NEPCM (nano-particle enhanced phase change material). A typical TES is phase change material which is explained in brief below.

A phase change material (PCM) is a substance which stores and releases large amounts of energy by virtue of latent heat energy. Heat is absorbed or released when the material changes from solid to liquid and vice versa; thus, PCMs are classified as latent energy storage units.

Phase-change materials (PCMs) allow large amounts of energy to be stored in relatively small volumes, resulting in some of the lowest storage media costs of any storage concepts. As such PCM's can be a potential candidate for storing thermal energy.

TAMU identified 2 eutectic mixtures and used them as the base TES material whose thermophysical properties were to be enhanced.

The compositions of the 2 identified eutectics are as follows:

1) The currently used Hitec solar salt: $NaNO_3 - KNO_3$: Molar composition of 46 % $NaNO_3$
2) Lithium-potassium carbonate: $Li_2CO_3 - K_2CO_3$ Molar composition of 42.7% Li_2CO_3

There have been several methods of improving the thermophysical properties of PCM's, one of which is by using nanoparticles. This enhancement has been termed as NEPCM (Nanoparticle Enhanced PCM). Choi et al. (3) have shown that NEPCM showed improved thermophysical properties (thermal conductivity) and have a great potential in thermal energy storage applications.

Typically, a CSP employs pipes and tanks to transport and store molten salt respectively. These pipes and tanks are made of steel. One of the factors determining the life of a CSP

(concentrating solar power) plant is the length of time these pipes and tanks can be used before they need replacing. This lifetime in turn determines amortized capital costs. As such studying corrosion and improving anti-corrosion properties may lead to a reduction in $/KWh at the system level.

Corrosion has a direct bearing on TES component life. From (4) corrosion has been reported to be a major issue. The pipes that carry the molten salt need to be corrosion resistant, otherwise they need to be replaced every year. Corrosion study becomes important as the containment technologies are required to last at least 30 years (5). The fact that the Solar Energy Research Institute has taken up a dedicated study of high temperature molten salt corrosion in TES containment materials shows the importance of corrosion, as it is the one of the most important factors deciding the life of a CSP plant. High temperature corrosion of steel in fused molten salt can be a significant source of concern (6).

1.1 Objective

My objective is to determine the effect of silica nanoparticles on the corrosion rate of SS304 stainless steel in molten carbonate eutectics under CSP conditions.

Why silica nanoparticles? TAMU developed nano-composite material (TES doped with a particular concentration of nanoparticles) which showed improvement in thermophysical properties in comparison with the base material. The nano-particles used were silica, titania, carbon nano-tubes and alumina. I chose silica nanoparticles as they showed the maximum improvement in thermophysical properties of the base carbonate

eutectic. By adding 1% by weight of silica nanoparticles, it has been shown that there is an improvement of 20% in thermophysical properties (7).

The objective was to measure the effect of adding silica nanoparticles to the molten carbonate salt on the corrosion of stainless steel 304(a material commonly used in CSP applications) under CSP conditions.

1.2 Background for the Hypothesis

Hypothesis: My hypothesis for this thesis is that silica nanoparticle reduce corrosion of steel SS304 by molten carbonate eutectic under CSP conditions.

Background: The thermophysical properties of TES were improved using alumina, silica, and titania nanoparticles. Previous studies conducted indicated a possibility of corrosion inhibition of steel by molten nitrate or carbonate eutectics by adding these nanoparticles to the molten salt.

The results of these tests indicated that addition of titania and alumina nanoparticles to the TES had a positive effect by reducing corrosion of steel. But nothing could be determined about silica nanoparticles effects. More importantly, since it was a preliminary test, the test methodologies were not based on any paper and were conducted purely as a preliminary investigation. Secondly, the uncertainty of these results was high. Though not conclusive, these tests provided a strong basis and motivation to investigate the effect of silica nanoparticles on corrosion of steel by molten carbonate eutectics.

2. THEORY

This section will detail the theory as regards to the hypothesis followed by the general corrosion mechanism focusing on molten salt corrosion and finally as theory applicable to experimental procedures focusing on mass loss and corrosion characteristics.

2.1 Theoretical Background for the Hypothesis

The driving force of corrosion is the lowering of free energy associated with the oxidation of a metal. Thermodynamics examines and quantifies this driving force. It predicts if reactions can or cannot occur (i.e., if the metal will corrode or be stable). It does not predict at what rate these changes can or will occur: this is the area of kinetics. However, knowing from thermodynamics what reactions are possible is a necessary step in the attempt to understand, predict, and control corrosion. Though this thesis will not be investigating the kinetics of such reactions, P.H. Suegama 2008 et al (2) have shown that silica nanoparticles induce reactions which reduce corrosion One way to improve the thermophysical properties of the molten salt is by adding silica nanoparticles and a useful byproduct of this addition is the expected reduction in corrosion.

From (8), molten fused salts are more corrosive than aqueous salt solutions. One of the ways to decrease the corrosion rate of molten salts is by reducing the oxidizing power of the salt with additives. In the TES project, these additives are nanoparticles whose primary objective is to improve the thermophysical properties of the salt. We hypothesize that these additives (nanoparticles) will also reduce the oxidizing power of the salt.

The metal subject to corrosion in this test is SS304, a material commonly used for containment in CSP plants. The typical composition of SS304 is Mn 2, Ni 9.25, Cr 19, Si 1, C 0.08, P 0.045, S 0.03, and Fe balance (9).

The proposed corrosive materials are the carbonate eutectic, with and without silica nanoparticles (1% by weight).

2.2 Corrosion and Its Mechanisms

Corrosion involves the interaction between a metal or alloy and its environment. Corrosion is affected by the properties of both the metal or alloy and the environment. The most important environmental variables include:

1) pH (acidity)
2) Oxidizing power (potential)
3) Temperature (heat transfer)
4) Velocity (fluid flow)
5) Concentration (solution constituents)

While corrosion obeys well-known laws of electrochemistry and thermodynamics, many variables that influence the behavior of a metal in its environment can result in accelerated corrosion or failure in one case and complete protection in another, similar case.

2.2.1 Mechanisms of Molten Salt Corrosion

Adler et al, (8)**,** have described two general mechanisms of corrosion can exist in molten salts. One is the metal dissolution caused by the solubility of the metal in the salt. This dissolution is similar to that in molten metals, but is not common. The second and most common mechanism is the oxidation of the metal, a mechanism similar to aqueous corrosion. For this reason, molten salt corrosion has been identified as an intermediate form of corrosion between molten metal and aqueous corrosion.

General, or uniform, metal oxidation and dissolution is a common form of molten salt corrosion but is not the only form of corrosion seen. Selective leaching is very common at higher temperatures, as are pitting and crevice corrosion at lower temperatures. All the forms of corrosion observed in aqueous systems, including stress-assisted corrosion, galvanic corrosion, erosion-corrosion, and fretting corrosion, have been seen in fused salts. Electrochemically, the molten salt/metal surface interface is very similar to the aqueous solution/metal surface interface. Many of the principles that apply to aqueous corrosion, such as anodic reactions leading to metal dissolution and cathodic reduction of an oxidant, also apply to molten salt corrosion. Based on this concept, recent studies have been successful in using electrochemical test methods commonly used in aqueous solutions (e.g., electrochemical noise, linear polarization, and harmonic distortion analysis) to make measurements of corrosion and localization in laboratory studies. This work has even been carried on to use in commercial plant operations to help relate changes in process variables to periodic conditions of accelerated corrosion (8).

The concept of acid and base behavior of the melt is very similar to that of its aqueous counterpart. The corrosion process is mainly electrochemical in nature because of the excellent ionic conductivity of most molten salts. Some investigators feel that dissolved water enhances the electrochemical corrosion nature of the molten salts.

Even though the corrosion mechanism is similar, there are major differences between molten salt and aqueous corrosion. The differences arise mainly from the fact that molten salts are partially electronic conductors as well as ionic conductors. This fact allows for reduction reactions to take place in the melt as well as at the metal/melt interface. This behavior also allows increase in frequency of cathodic reactions and can therefore lead to a substantial increase in corrosion rate over a similar electrochemically controlled aqueous system, especially if the corrosion media contain very few oxidants. Because of property differences between water and molten salt, the rate-controlling step in most molten metal systems is ion diffusion into the bulk solution, not the charge transfer reaction that is typical of aqueous systems. Molten salt systems operate at higher temperatures than aqueous systems, which lead to different forms of corrosion attack.

Electrochemical measurements have highlighted these differences between aqueous and molten salt environments, particularly in terms of characterizing their polarization through the classical Stern-Geary relationship. Values obtained in a molten salt system tend to be much different than those observed in an aqueous system, brought about by the simultaneous presence of many ionic species and the combined ionic and electronic conduction mechanisms in molten salts. However, use of these techniques has resulted in

meaningful measurement of corrosion rates that correlate with actual mass losses in system components in combustion environments (8).

The paourbaix diagram (Figure 1) explained next explains possible corrosion reactions for iron corroding in a molten carbonate salt. This diagram is key to understand the corrosion dynamics.

Paourbaix diagram of Iron in molten carbonate Salts (taken from (10) Watanbe et al):
The regions of immunity, corrosion and passivation of a metal in aqueous solutions can be assessed from the so-called Pourbaix diagram (potential-pH diagram). Bearing in mind that the oxygen anion is most likely to be reduced during the partial cathodic reaction, potential - pO^{2-} diagrams were devised in analogy to this treatment for a range of metals in molten salt electrolytes to define the zones of corrosion and passivation. It is known that the dissociation of oxygen-containing anions gives rise to a well-defined acid-base behavior.

$SO^{2-}_4 \longrightarrow SO_3 + O^{2-}$ ---------- (1)

$NO^{3-} \longrightarrow NO^{+}_2 + O^{2-}$ ---------- (2)

$CO^{2-}_3 \longrightarrow CO^{2-} + O^{2-}$ ---------- (3)

$2OH^- \longrightarrow O^{2-} + H_2O$ ---------- (4)

In accordance with the Lux-Flood theory, mentioned in Watanbe et al (10), oxygen containing anions acts as a base in the supply of oxide anions and the corresponding gas oxides are their conjugate acids. From the above equilibria it follows that the acidity of the melt may be expressed by pO^{2-}. Accordingly, the E/pO^{2-} diagram provides a suitable

framework for determining passivation zones and the electrochemical behavior of different metals. This passivation zone is considered a direct measure of the amount of corrosion which in turn determines the corrosion rate. Thus removing the passivated layer and normalizing with time will lead to corrosion rate. This method of determining corrosion rate by removing the passivating layer is termed as 'gravimetric or mass loss' method of determining corrosion rate.

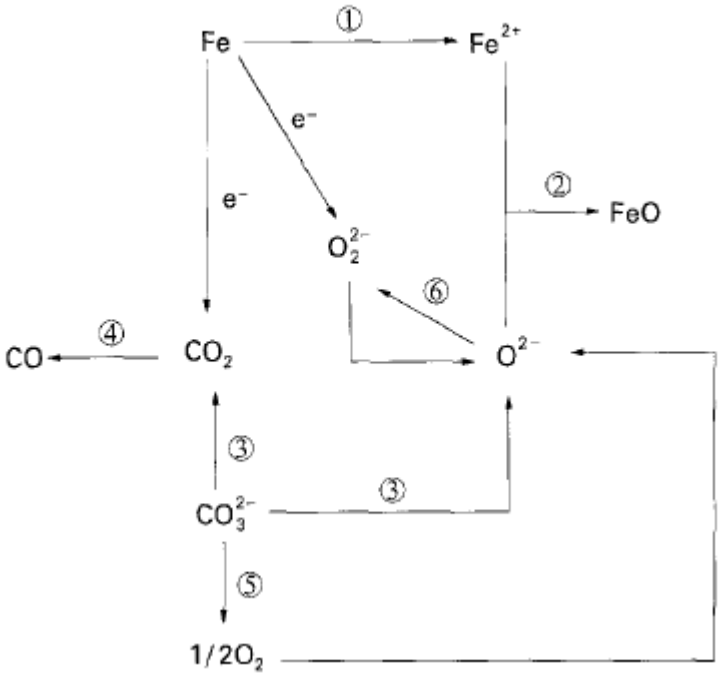

Figure 1: Paourbaix Diagram: Summary of the Electrochemical Corrosion Reactions of Iron in Carbonate Melts (Taken from Watanbe et. al (10)).

In the diagram, the carbonate anion breaks as in reaction 3. This provides O^{2-} for oxidation/corrosion of Iron. It is expected that nanoparticles will reduce the oxidizing

power of the melt and hence form adducts. An adduct is a chemical compound that forms from the addition of two or more substances. The adduct forms a passivating layer and inhibits corrosion (2). It is expected that silica nanoparticles will form a passivating layer by forming an adduct which is stable and also this adduct is formed by transforming less parent material compared to the adduct formed without silica nanoparticles. On descaling, the mass loss normalized with time and area will be a direct indicator of the corrosion rate.

The next section talks about the theory as applicable to the experimental procedures and the expected corrosion characteristics.

2.3 Thermodynamics and Kinetics of Chemical Oxidation of Metals

Market Research Report (4), has reported that the thermodynamic feasibility of a corrosion reaction is determined by the change in free energy of the system during corrosion process.

$Me + 1/2O_2 \leftrightarrow MeO$

However, such determinations can also be made by comparing the dissociation pressure of the oxidation product and the partial pressure of Oxygen. If partial pressure of Oxygen is less than dissociation pressure of the oxidation product the backward reaction progress and vice versa. Corrosion takes place if the forward reaction is favored forming an oxide film.

Conditions for film Continuity is determined as follows. Let V_{Ox} be the volume of oxide formed and V_{Me} be the volume of the metal. If $V_{Ox}/ V_{Me} > 1$genearlly form films with good protective properties.

Film Growth exhibits 3 patterns. There are 3 laws of film growth:

1) Linear Law

2) Parabolic Law.

3) Logarithmic Law.

Linear Law: here $V_{Ox}/ V_{Me} < 1$ we have $dy/dt = K$ where y is the film thickness. This implies "y" is proportional to the oxidation time.

$Y = Kt + A;$

All alkali metals undergo this type of corrosion.

Parabolic Law:

$y^2 = Kt + A:$

Here $V_{Ox}/ V_{Me} > 1$, the corrosion process will be retarded by diffusion of corrosion products through the film. This results in thickening of film which continuously decreases the corrosion rate with time.

Iron oxides typically observe a parabolic law of film growth. Elements that also follow this growth pattern are Cu, Fe, and Ni.

For iron the expected rate of corrosion is parabolic (11)**.** The expected parabolic behavior is seen in Figure 2.

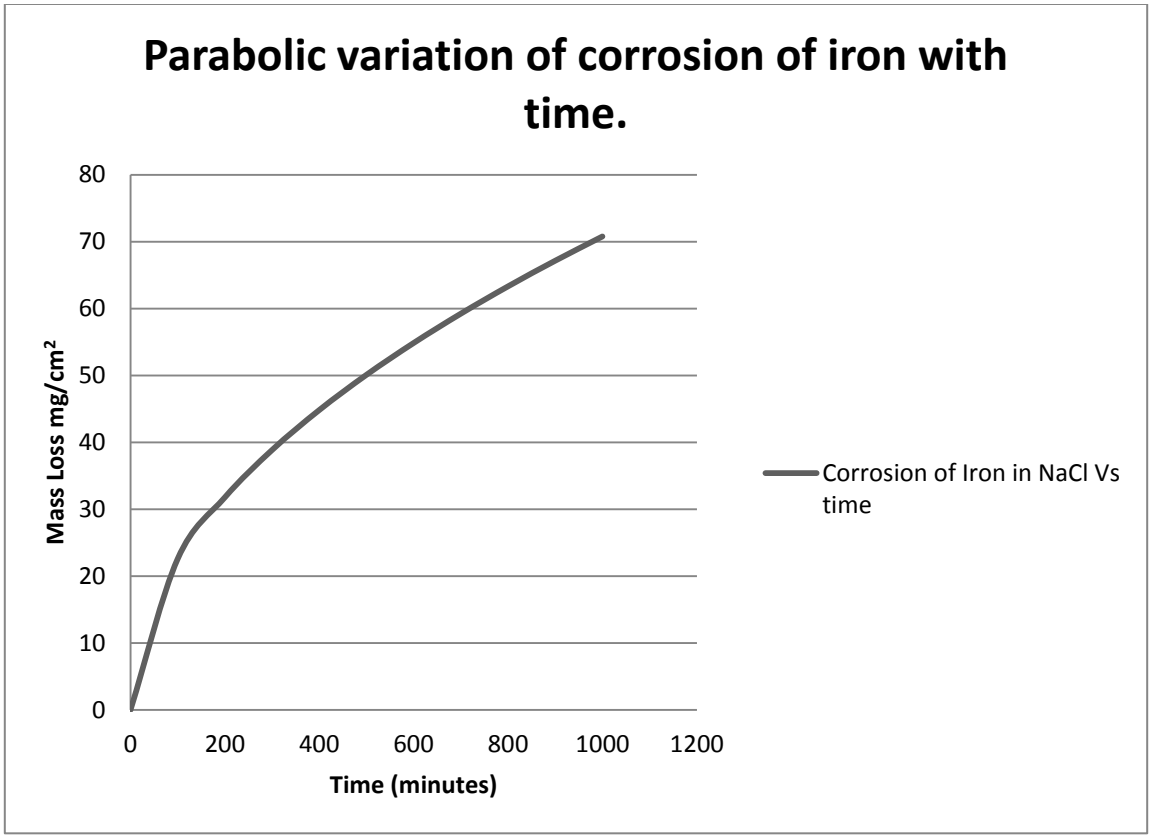

Figure 2: Corrosion Characteristics of Iron with Time (11).

Logarithmic Law: This type of film growth is characterized by a much slower growth than predicted by parabolic law.

The film thickness is expressed as

$y = \ln (Kt)$

The growth rate is

$dy/dt = K/e^{y}$

Al, Cr and Zn undergo logarithmic law. Iron in particular follows a logarithmic law up to 400C and a parabolic law from 500C to 1100C.

Mass loss and Corrosion are determined as follows. As discussed, the film growth on the surface due to corrosion is a result of the transformation of the base metal into oxides. The term mass loss indicates the mass of transformed metal into oxides. Thus, mass loss provides a way to measure corrosion rate. Mass loss is one way to quantify the corrosion rate. Normalized mass loss per unit area per unit time is a very good indicator of the rate of corrosion. Molten salt corrosion rates are predominantly determined using gravimetric mass loss (8). Other quantifying techniques include electrochemical noise, linear polarization, and harmonic distortion analysis. Only mass loss will be used in this thesis.

Rate of corrosion- Corrosion is an electrochemical process and there are several ways to quantify the rate of corrosion. Ideally, rate of corrosion is measured using an electrochemical cell, where the metal whose corrosion rate is to be determined is set up as the anode and the corroding environment/ agent is the electrolyte and the corrosion product is formed at the cathode. The corrosion current is directly proportional to the rate of corrosion. The concept of Polarization potential is also used in determining the rate of corrosion. The corrosion rate follows a Gaussian distribution and it is said that a Gaussian distribution describes the corrosion rate the best (12).

In addition to the above methodologies, the concept of mass loss (anodic mass loss) directly measures the rate of corrosion. As the experimental setup demonstrates, the anode and cathode are essentially the same steel coupon, and the surrounding molten salt acts as corroding environment and completing the electrochemical circuit. So after the

experiment, when the steel coupon is descaled with hydrochloric acid, it removes all the oxides formed and leaves the steel coupon alone. This method has been detailed in (9)**.**

Bradshaw et al have shown that the time of exposure to the environment must be large enough to capture oxide-metal interface. The average time of exposure is about 300-1000 hours.

The rate of corrosion can be used to identify and classify the operability of steel into various categories. This classification per Cabeza et. al (13) will be used as a basis to give recommendations to DOE. This table of classification is as below (Table 1).

Table 1: Corrosion Rate and their Operability in Industries. (13)

Corrosion Rate: mg/cm^2/yr.	**Corrosion Rate mm/yr.**	**Recommendation**
> 1000	>2	Completely destroyed within days
100 to 999	0.2 - 1.99	Not recommended for service greater than a month
50 to 99	0.1 - 0.19	Not recommended for service greater than one year
10 to 49	0.02 - 0.09	Caution recommended, based on the specific application
0.3 to 9.9	NA	Recommended for long term service
< 0.2	NA	Recommended for long term service; no corrosion, other than as a result of surface cleaning, was evidenced

3. EXPERIMENTAL METHODS

The conceptual design: The experiment was designed to mimic the wall conditions of the steel container used as storage tanks in a CSP exposed to molten carbonate eutectics. This was achieved using a coupon made of SS304 (material used for constructing a storage tank of a CSP). This coupon approximately 5X20X.6mm and .5gms in weight symbolized the wall of a storage tank (Figure 3).

The Figure 3 below is a schematic diagram of the coupon.

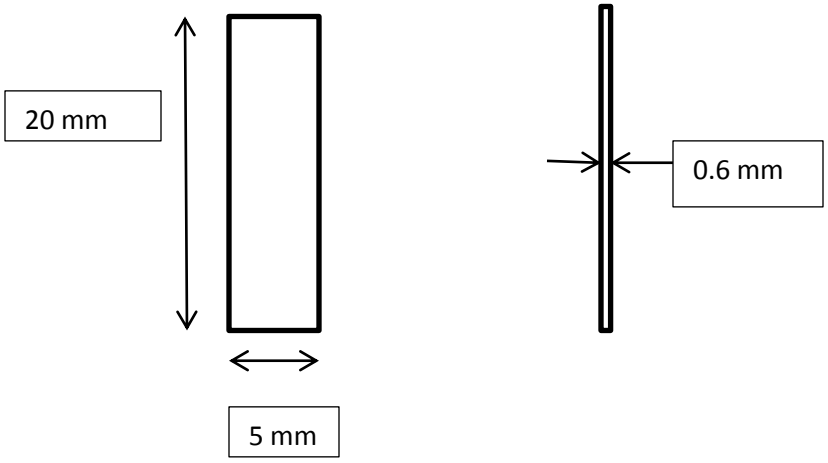

Figure 3 A Schematic Diagram of a Steel Coupon.

This experiment was a static immersion test, implying that the corroding environment (molten eutectic) would be static and always in contact with the steel coupon. The

temperature for testing was set at a constant 520C a temperature comparable to those encountered in a CSP.

The following experimental set-up was used to best mimic the walls of a storage tank of a CSP. A ‘sample bomb’ design was adopted. A sample bomb is essentially a steel tube 3/8” in diameter and 3” in length filled with a steel coupon surrounded by a TES material and sealed at both ends using compression fittings. This is schematically shown below. The highlighted portion in the image is depicted using the schematic diagram. Note that the image contains multiple sample bombs assembled together. The schematic shows just one sample bomb, as such one of the sample bombs in the assembly (image) must be compared with the schematic diagram of the sample bomb. Figure 4 below is a schematic representation of the sample bomb assembly.

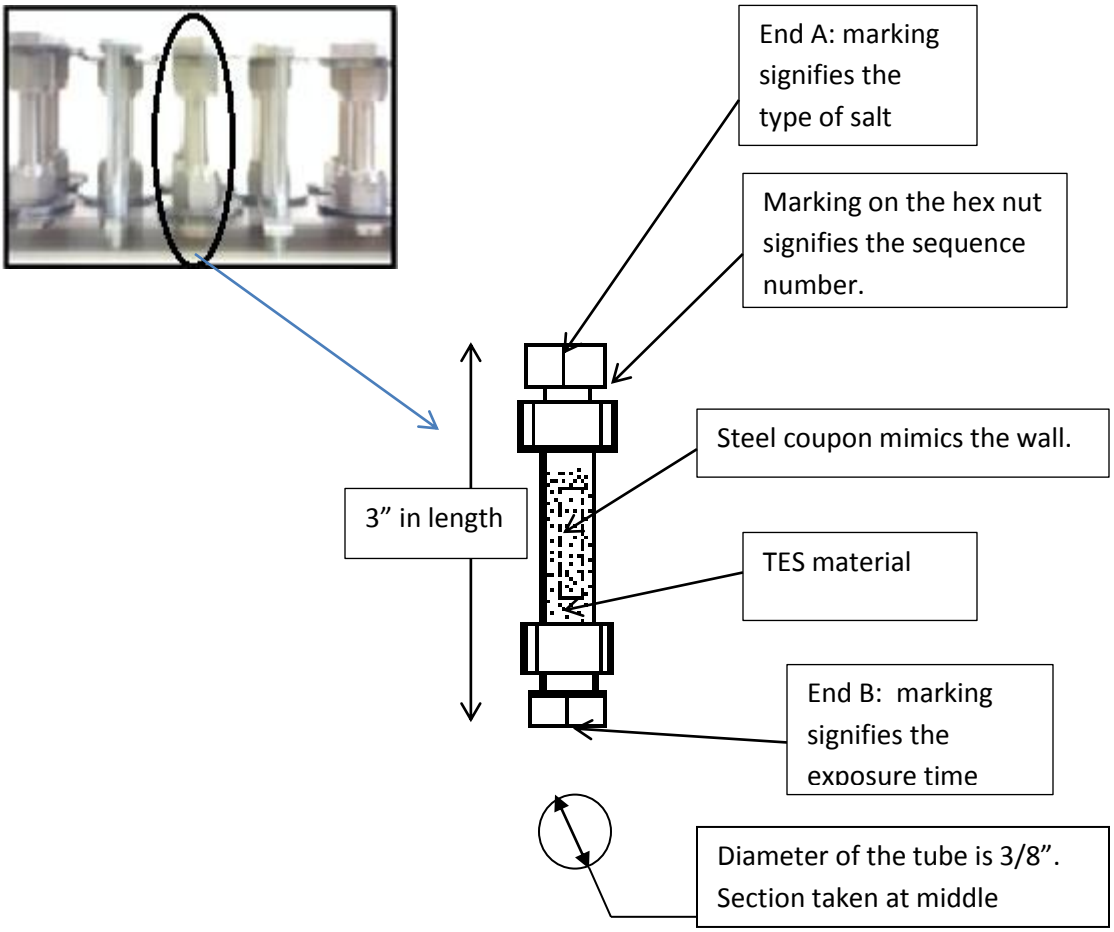

Figure 4 A Schematic of Sample Bomb with Reference to an Actual Sample Bomb Photograph.

From the Figure 4 the following can be observed,

1) The sample bomb has 3 markings for it to be uniquely determined.

2) The top side labeled as ‘A’ indicates the type of salt.

The bottom side labeled as ‘B’ indicates the duration of the test. These are detailed after explaining marking ‘A’. The marking on the nut on the top side (side where salt type is marked) contains marking to indicate the sequence number between 1 and 3. This is done because there are 3 samples per salt per timeframe. This sequence number is

important to uniquely identify a sample bomb from the rest of the sample bombs of the same family. Here the term family means a particular type of salt and a particular exposure time. There are 3 per family. The concept of sequence numbers will be clear as the reader progresses through the sections.

The salt marking on the top end A are as follows (Figure 5).

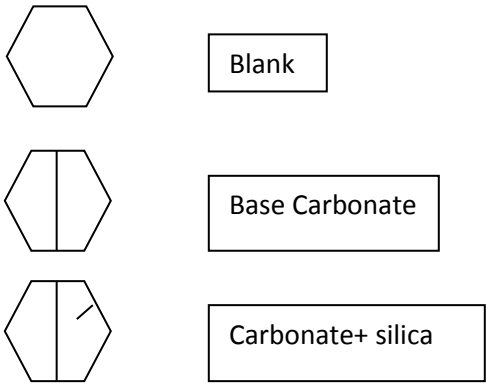

Figure 5: Type of Salt Indicators.

The salt marking on the top end B are as follows (Figure 6).

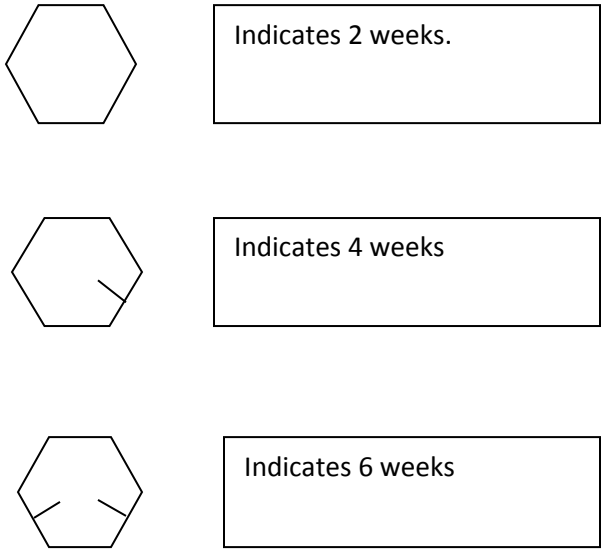

Figure 6: Exposure Time Indicators.

The test matrix: Each cell in the test matrix gives the number of samples per exposure time. This is depicted in Table 2.

Table 2: Test Matrix

Salt→ Time(wks)	Carbonate	Carbonate+Silica	Blank	Total/Time
2	3	3	3	9
4	3	3	3	9
6	3	3	3	9
			Total	27

As can be seen, there are 3 samples per family. This means there were three sample bomb assemblies per corroding environment and exposure time. This was done to establish confidence in results.

The term blanks signify corrosion without any corroding environment. This was to act as a baseline. Blanks are sample bombs without any TES material.

After finalizing on the design, the parameters for the experiment are presented next.

3.1 Parameters for Experiment

The following parameters were set:

1) The time for corrosion must be significant to have measurable mass loss. This was taken to be in the order of hundreds of hours as per Thomas et al (8) and Tzvetkoff et al (14). Accordingly a timeframe of 300-1000 hours (2to 6 weeks) was chosen.
2) Ideally a larger surface area yields a better result. This is because a larger surface area will provide a larger mass loss and a larger mass loss will reduce uncertainty in the results. However, a larger surface area is constrained by the amount of salt

available, the furnace size, and cost. Given these constraints the best option was to adopt a steel coupon design with dimensions of approximately 20x5x.6 mm. Both (10), (8) suggest a steel coupon design. In addition the size above matches those used in testing by Bradshaw et.al (9)).

3) The minimum quantity of salt was determined by the need to completely cover the steel coupon in molten salt.
4) The steel tubing (which was used as a housing to contain the steel coupon and the salt) length was determined by the size of the oven, which in turn set the maximum size of the coupon and the amount of salt.
5) The steel tubing length must also account for volume expansion, which is approximately 18% for the carbonate salts.
6) The temperature of testing was set at 520 C, a temperature that was comparable to those used in CSP operations (500-600C) and above the melting point of the carbonate eutectic.
7) The posttest cleaning: The posttest cleaning process of coupons was done according to the procedure detailed in Bradshaw et.al (9) and Watanabe et.al (10). According to those papers, the gravimetric mass loss was obtained by using concentrated HCl to descale the corroded coupons. A time of 1 minute was determined to be sufficient from previous tests.
8) Once descaled, the time and area normalized mass loss gave the actual corrosion rate.

Experiment design consideration is described next. In this section, I talk about the reason behind adopting a particular parameter discussed above. In addition to providing a

qualitative explanation of the reason for choosing the parameters, I also highlight certain additional requirements on the experimental process.

3.1.1 Controlled Parameters

The controllable parameters include:

1) Steel coupon size.
2) Amount of salt.
3) Exposure time in the salt.
4) Time duration of HCl acid exposure for descaling.
5) Time required to remove the steel coupon from the sample bomb (Here the term sample bomb is steel tubing that contains the steel coupon surrounded by the TES material sealed at both ends by compression fittings. Refer Figure 3.)
6) Concentration of silica nanoparticles kept at 1% by weight.
7) Temperature of the test.
8) Orientation of the sample bomb.

Steel Coupon size: In this experiment, experimental procedures were based on experimental procedures detailed in Cabeza et al. (13) and Bradshaw et al (9). The average weight of the steel coupon was around 0.5 gms. Their dimensions were 5x20x.6 mm.

Corrosion is a surface phenomenon and area is believed to have a significant effect. Keeping this in mind, the area of the samples was kept nearly uniform. More

importantly, results were normalized to the surface area of the coupon, removing dependency on steel sample surface area.

Amount of salt: The amount of salt was chosen based on the requirement that the salt completely cover the steel coupon inside the sample bomb. This was necessary to remove any effects of confounding due to insufficient exposure between the coupon and the corroding environment.

Time duration of the experiment: Literature survey indicated that steel specimen subject to corrosion must be for a sufficiently long time to have observable effects. According to Bradhsaw et al (9) and Cabeza et al (13), the time frame of 2 and 6 weeks were considered.

Time duration of HCl acid exposure for descaling: Descaling is a process of removing soluble oxides. Hydrochloric acid was used for descaling. Hydrochloric acid was used for descaling because the process for descaling by Bradshaw et al (9) also used hydrochloric acid. It is important that all possible causes of variability be mitigated. In order to achieve this, the following was kept as a guideline:

1) Time each descaling process with a stopwatch.
2) Rinse the coupon immediately to remove acid.
3) Weigh it immediately post descaling.
4) Ensure a new quantity of hydrochloric acid for each new sample, to ensure that all samples are subjected to the same strength of hydrochloric acid.

With these measures, it is hoped that any normalized area and time gravimetric change will be solely due to dissolution of soluble oxides and thereby giving a direct indication of amount of corrosion.

Time duration of removal of the steel coupon from the Sample bomb: The sample bomb assembly (steel tubing sealed at both ends along with the steel coupon and salt inside it), after removal from the furnace needs to be opened to remove the steel coupon.

From past experience, it was observed that removing steel coupons sometimes may prove difficult. This difficulty happens when the salt seals the steel coupon with the wall of the steel tubing. In order to remove the steel coupon, the open end of the sample bomb was immersed in distilled water. This process took a couple of days for the distilled water to soften the molten salt after which the steel coupon could be removed.

Concentration of Silica Nanoparticles: The concentration of silica nanoparticles was 1% by weight throughout the experiment.

Temperature of test: The temperature of the test was maintained at a constant temperature of 520C. There was no significant variation of temperature. The actual observed variation in temperature was found to be about ±5C. This variation was measured initially before the experiment using a thermocouple at regular intervals of one hour for 6 hours.

Orientation of the sample bomb: The sample bomb was to be kept vertical to ensure that the steel coupon was in constant contact with the molten carbonate salt. Hence a frame was built to ensure that these sample bombs were always upright during the test.

3.1.2 Uncontrolled Parameters

The uncontrolled parameters were

1) The amount of physical cleaning after descaling.
2) Uniformity of temperature in the oven.

The amount of physical cleaning: The steel coupon after descaling is rinsed with distilled water and immediately wiped dry with wipes. The amount of physical cleaning is highly subjective. I standardized the procedure by wiping the steel coupon just once in one direction. This will prevent any biasing of results due to physical cleaning.

The uniformity in temperature in the oven: As stated above, the temperature variation in the furnace was a maximum of ±5C with temperatures ranging from 520±5C. This means that the salt was in the molten state at all times, since the melting point of the carbonate eutectic is 488.8C. Also, since all samples were subject to the same variations any biasing due to such variations could be ignored.

The next section details the experimental process or the methods employed to conduct the test. This was the procedure followed, keeping the parameters and the design considerations in mind.

3.2 Experimental Process/Methods

All experimental processes have been in accordance with the ‘parameters for experiment’ and design considerations. Past experience also provided a basis for establishing a more reliable and confident procedures. Procedures were tailored to best fit/satisfy the design considerations. The process below describes what was done. Each of these processes will be further drilled down chronologically in the sections that follow.

The experimental process was to set up an environment for hot chemical corrosion of SS304 by molten salts that will simulate CSP conditions. The experimental setup simulated CSP conditions using the sample bomb design. A ‘sample bomb’ in our case is essentially a 3/8” steel tubing approximately 3” in length containing a steel coupon, surrounded by a TES material and sealed at both ends (Figure 3). Here a steel coupon (the same grade steel used to construct storage tanks and pipes used to contain and carry salts respectively) was immersed in a dry TES material filled inside a sample bomb in argon atmosphere (to exclude other oxidizing agents). The steel coupon mimics the wall of a storage tank or the wall of pipe.

A survey of the literature indicated that steel specimens subject to corrosion must be immersed for a sufficiently long time to have observable effects (14)**.** Keeping this in mind, the time frame of 2, 4 and 6 weeks was considered. The sample bomb was then placed in the furnace for testing. The temperature of testing was set at 520 C. At all times, the sample bomb was kept in upright position with the help of a frame to ensure

the coupons were submerged in the molten salt at all times during the test. Blanks (sample bombs with no TES material) were also tested and were used as baseline measurements for comparing corrosion rates. These sample bombs (banks) would be directly placed inside the furnace unlike the rest, which were positioned using a frame. After the completion of the required exposure time, the sample bombs were removed from the furnace. They were then opened to remove the steel coupon inside. Once the steel coupon was removed, it (steel coupon) was subject to coupon handling. The coupon handling has been detailed in the subsection 3.2.4. The final stage in coupon handling is descaling.

The steel coupon was descaled using hydrochloric acid and massed. This descaling is done to remove the oxide layer formed which directly indicates the amount of corrosion.

The basic experiment can be divided into four sections as detailed below.

3.2.1 Material Preparation

The experimental process consisted of salt and steel coupon as the basic material to perform these tests. The sections below detail the preparation of each.

3.2.1.1 Salt Preparation.

The salts were prepared using the aqueous method. The following sequences of steps were carried out:

1) The base salt Lithium-Potassium Carbonate) in combination with the nanoparticle silica was used as salt for this experiment/study. Nanoparticle concentration was 1% by weight throughout.

2) Past experience dictated that a sufficient quantity of material be used to cover the entire volume and also ensure a high salt mass to sample mass ratio. This requirement translated into 120gms of material for each type of salt. Here a type of salt means either a base salt or the nano-composite salt.

3) Salts were prepared using the aqueous method. Salt (Base salt +Nanoparticle) was first dissolved in water. It was then subject to rapid evaporation, ensuring a nice fine fry powder at the end of evaporation. To speed up the process large vials (capacity 4 oz) were used to dissolve the salt in water. The process can be detailed further as follows

    a) The salt and the Nanoparticles were mixed in the glove box with Nanoparticles being 1% concentration by weight. To this (1 gm of mixture; mixture indicates Salt+ nanoparticles) was added 100 ml of distilled water.
    b) The solution (salt and distilled water) was then sonicated for 3-4 hours.
    c) After sonicating, the solution was then transferred to evaporating dish and evaporated in the glove box. This, on an average took 45 minutes.
    d) After evaporation, the salt was scrapped off from the evaporating dish and then transferred to a clean dry vial and labeled.

The material was prepared in bulk. It was this bulk material that was used for the test. The method of preparation was the same as that those detailed in the points above,

except that the process was scaled up to produce a total of 120gms each. (Silica + carbonate eutectic)

3.2.1.2 Steel Coupons

The steel coupons were cut from the SS304 steel sheet. The dimensions of these were approximately 20x5x.6 mm. These steel coupons mimic the walls of a storage tank and pipes. Each coupon was marked and stamped with a number ranging from 0-44. This was done to ensure correct association of each coupon with the salt and timeframe of the experiment.

3.2.2 Sample Bomb and Frame Design

The sample bomb and frame were essential testing aids and are required auxiliary components to complete the test successfully. They helped in simulating actual CSP conditions. Hence these are described below.

The sample bombs were made of compression fittings and 3/8" tubing.

1) The steel tubing was cut into sizes of approximately 3".
2) The tube was then sealed at one end using compression fittings.
3) After filling them with salt and the steel coupon, these were then sealed at both ends with help of Swagelok compression fittings. The sealed steel tubing with salt and steel coupon with no oxidizing environment is called a sample bomb.
4) A total of 45 sample bombs were created. Each of the sample bombs were marked with appropriate signs to indicate
    a) The composition of the salt.

b) The duration of the test. (All markings were done using hand tools).

In order to reduce uncertainty we used 3 samples per salt per time of exposure. The sample bombs, thus had a marking for the type of salt and one more to indicate the sequence number (This number indicates sequence number for particular salt and timeframe).

The design considerations cited the importance of ensuring that the sample bombs be kept vertical to ensure contact of the molten salt with the steel coupon. The frame provided a slot for each sample bomb. The frame was designed so that it could provide an easy way to slide the sample bomb and then the entire assembly (group of sample bombs) could be assembled as a single unit.

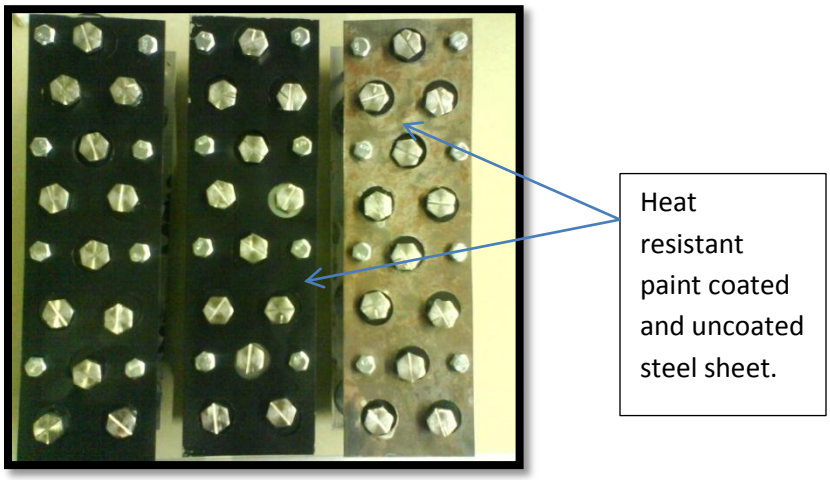

Figure 7: A Photo of Assembled Sample Bombs in the Frame.

The Figure 7 above shows two frames painted with heat resistant coating. This was done to prevent welding the Swagelok fittings to the frame. The other frame is yet to be coated and was coated later. The figure above is to show the appearance of the frame before and after coating with the heat resistant paint.

3.2.3 Testing

This section details from the assembly of a sample bomb until the removal of the sample bomb from the furnace after testing. The testing can be described as follows (refer to Figure 2 for all notations).

1) The cleaned steel tubing, loose fittings, steel coupon, washers and the salt were kept inside an argon circulated glove box.
2) The steel tubing was sealed at end ‘B’ using a compression fitting. It was then fitted with a washer at end ‘B’ and hand tightened at that end.
3) Then, the end ‘A’ was opened and filled with 3-4 small scoops (of size equal to half a teaspoon) of TES material.
4) The appropriate steel coupon was then inserted into the open end ‘A’ lengthwise.
5) The tube was then filled with salt to 75% of the length of the steel tubing.
6) The end ‘A’ was then fitted with a washer and then closed with hexagonal nut and hand tightened.
7) Each of the sample bombs were then tightened at end ‘B’ using a wrench and the top end ‘A’ was just slightly tightened. The ‘slight tightening’ requirement at end ‘A’ facilitates easy removal of steel coupons after the test.

8) This process 1 through 6 completes one complete assembly of a ‘sample bomb’. All together 27 such sample bombs, including blanks, were created. The only difference in the blank being there was no salt added.
9) The test samples (complete assembly) totaling 27 in number were then segregated according to timeframes (2, 4 or 6 weeks). This led 9 for each timeframe. The blanks which had no salt did not need to be kept vertical. Thus these were directly placed inside the furnace and not in the frame.
10) The remaining 6 samples per each timeframe were assembled in the frame.
11) A total of 3 frames, each containing 6 samples were then assembled.
12) The assembled frame was then placed inside the furnace as can be seen in Figure 8.

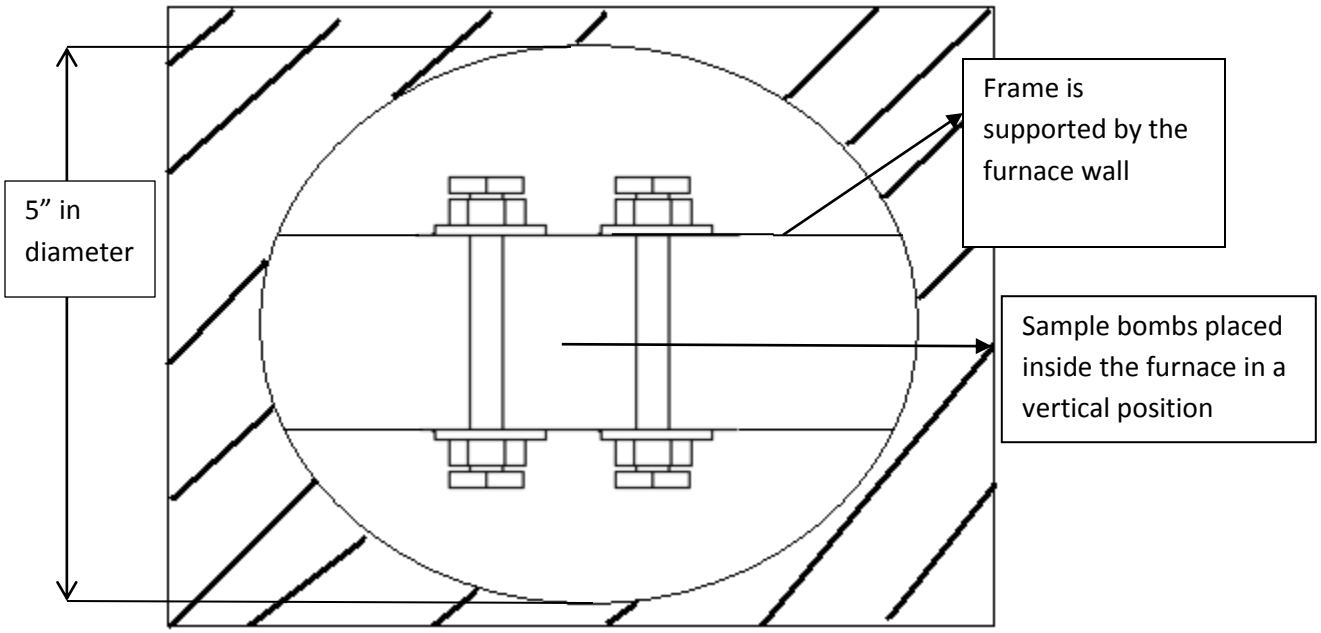

Figure 8: Schematic Diagram of the Placement of the Assembled Frame Inside the Furnace. Front View of the Furnace.

13) As can been seen above, the samples are held vertical at all times. The frame was stiff enough to withstand thermal loading and did not warp ensuring a vertical position for all samples at all times.
14) At the end of each exposure time, the corresponding frame was removed and so were the corresponding blanks.

3.2.4 Coupon Handling

After the frames were removed from the furnace, the sample bombs were removed from frame. Each tested sample bomb was then subjected to the following processes.

3.2.4.1 Coupon Removal

The tested sample bomb is opened at end 'A'. After opening at end 'A', the opened sample bomb is then placed inside a vial containing distilled water. The distilled water then softens the solidified salt and in the process loosens the steel coupon for removal. This may take from 2 days at a maximum. Once the salt is softened, the steel coupon settles at the bottom of the vial to be collected.

3.2.4.2 Coupon Cleaning

After the coupons are removed from the vial, they are then subject to cleaning by distilled water and wipes to remove any traces of salt. These are then dried, labeled and put in vials, ready to descale.

3.2.4.3 Measurements

The coupons obtained from the above stage were then subject to descaling to obtain the mass loss. The descaling process is done using concentrated hydrochloric acid. Each dry

coupon is immersed in a concentrated hydrochloric acid for precisely one minute. They are then cleaned and dried with wipes and then immediately weighed in a microgram balance. Results are recorded in an Excel containing the previously determined mass measurements data. The difference between the two directly yields the mass loss data. These are then surface normalized and analyzed.

4. RESULTS

The mass loss data obtained from Experiments are surface and time normalized to obtain the corrosion rate. These are then compared (between salts doped with and without silica) and plotted against time.

As discussed earlier, a total of 27 tests samples were tested with three per salt and timeframe. Referring back to the objective, the results and their discussions presented here will be presented with an objective to compare the rate of corrosion of steel with and without silica nanoparticles. The data will be pivoted in different ways to help analyze and verify any findings that supports the initial hypothesis. The results will be presented in the following sequence.

Corrosion Rate (determined at specific times):

1) Carbonate 2 week and Carbonate Silica 2 week.
2) Carbonate 4 week and Carbonate Silica 4 week.
3) Carbonate 6 week and Carbonate Silica 6 week.
4) Carbonate Total Comparison: To verify the corrosion characteristics of steel.
5) Average corrosion rate (averaged over all exposure times).
6) Relative comparison of corrosion.
7) Statistical Analysis.

The rate of corrosion is given as gms/ cm^2/day and the exposure time in weeks. Each bar is an average of the instantaneous corrosion rates for that particular salt and that exposure time. As explained earlier, there were 3 samples per corroding material and per

exposure time. Thus each sample gives an instantaneous corrosion rate. These 3 instantaneous corrosion rates are averaged to determine the average instantaneous corrosion rate. This value is plotted in the bar graph (Figures 9, 10 and 11).

The results also include the total corrosion comparison, wherein the corrosion data is only area normalized. Total corrosion differs from mean instantaneous corrosion rate in the sense that they are only area normalized and not time normalized. Total corrosion refers to the value that is the mean of corrosion rates normalized with respect to only area of the three samples per corroding environment and per exposure time. This comparison was done to compare the observed behavior of the corrosion with the predicted model for corrosion in ferrous materials.

4.1 Plain versus Doped Results

The results below compare the corrosion rate of steel by molten plain and doped carbonate salts at 2,4 and 6 weeks. Each of the corrosion rates are obtained by averaging 3 data points. The uncertainty bars indicate the standard deviation from the mean.

The uncertainty ranges from 7-10%. To establish further confidence in the shift of means due to doping a t test was performed. There is a 95% confidence in the results that the mean has shifted in the direction of reduced corrosion due to doping. This test has been detailed in section 4.4

4.1.1 Comparison of Corrosion Rates between Carbonate and Carbonate Doped with Silica Nanoparticles 1 % by Weight

Figure 9 shows the average corrosion rate by carbonates and carbonates doped with silica. The figure was created by averaging the normalized mass loss rates for each salt type. Figure 9 shows the results for 2 weeks, Figure 10 for 4 weeks, and Figure 11 for 6 weeks.

Figure 9 indicates that due to doping, the corrosion rate has decreased by about 40% in comparison to the corrosion rate without doping. There is 95% confidence level in this claim.

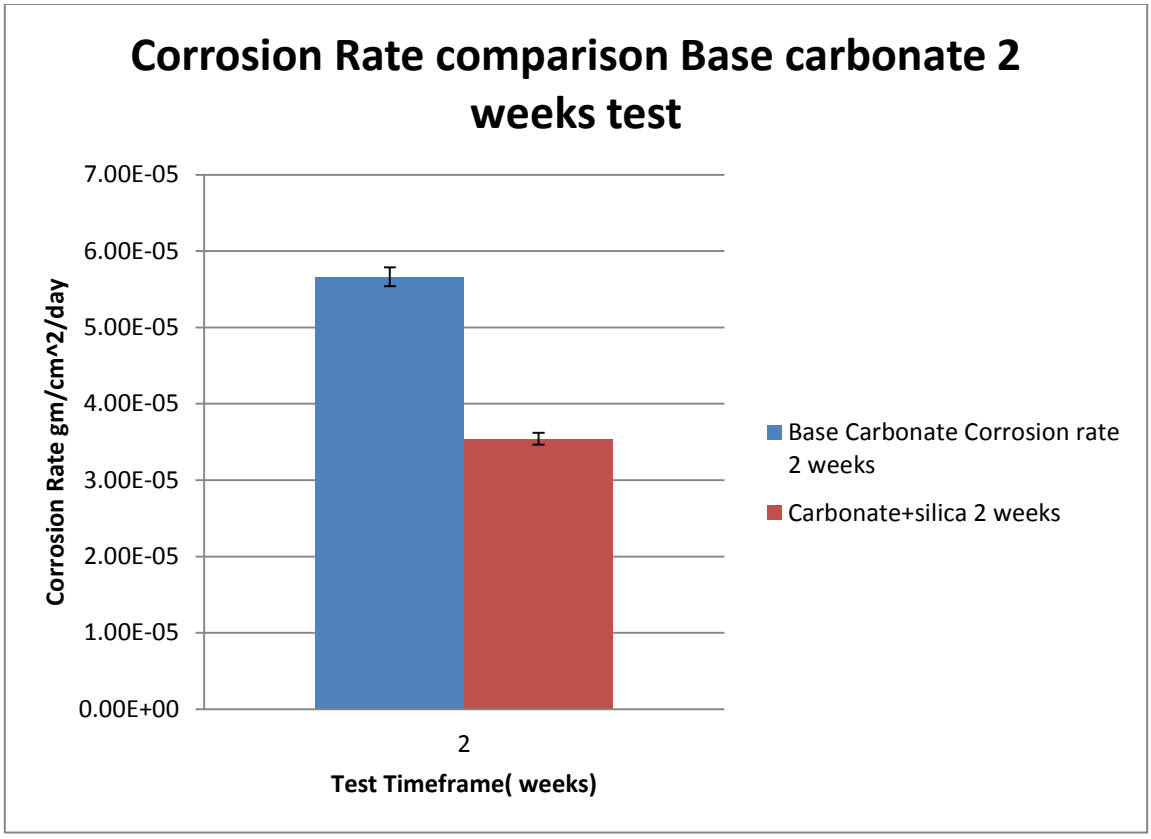

Figure 9: Instantaneous Corrosion Rate Comparison between Carbonate and Carbonate Doped with Silica at 2 Weeks.

Figure 10 indicates that due to doping, the corrosion rate has decreased by about 65% in comparison to the corrosion rate without doping. There is 95% confidence level in this claim.

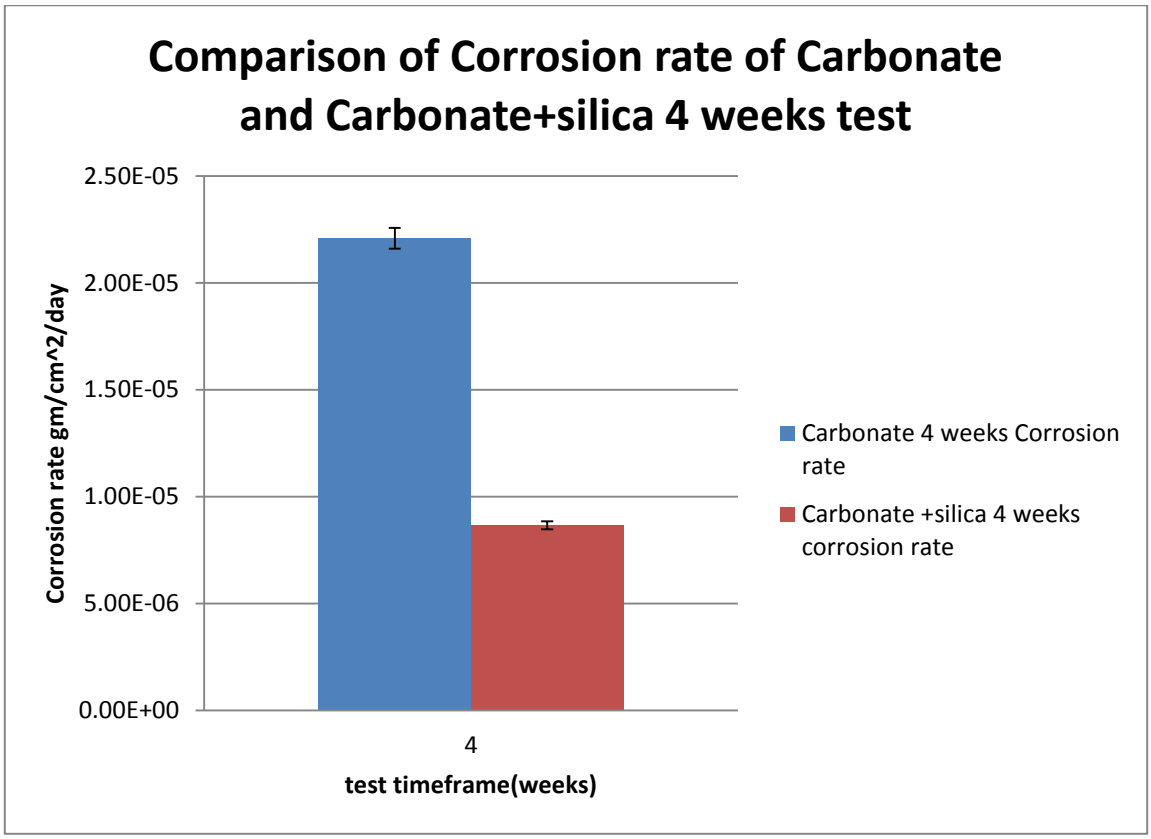

Figure 10: Instantaneous Corrosion Rate Comparison between Carbonate and Carbonate Doped with Silica (4 weeks).

Figure 11 indicates that due to doping the corrosion rate has decreased by about 50% in comparison to the corrosion rate without doping. There is 95% confidence level in this claim.

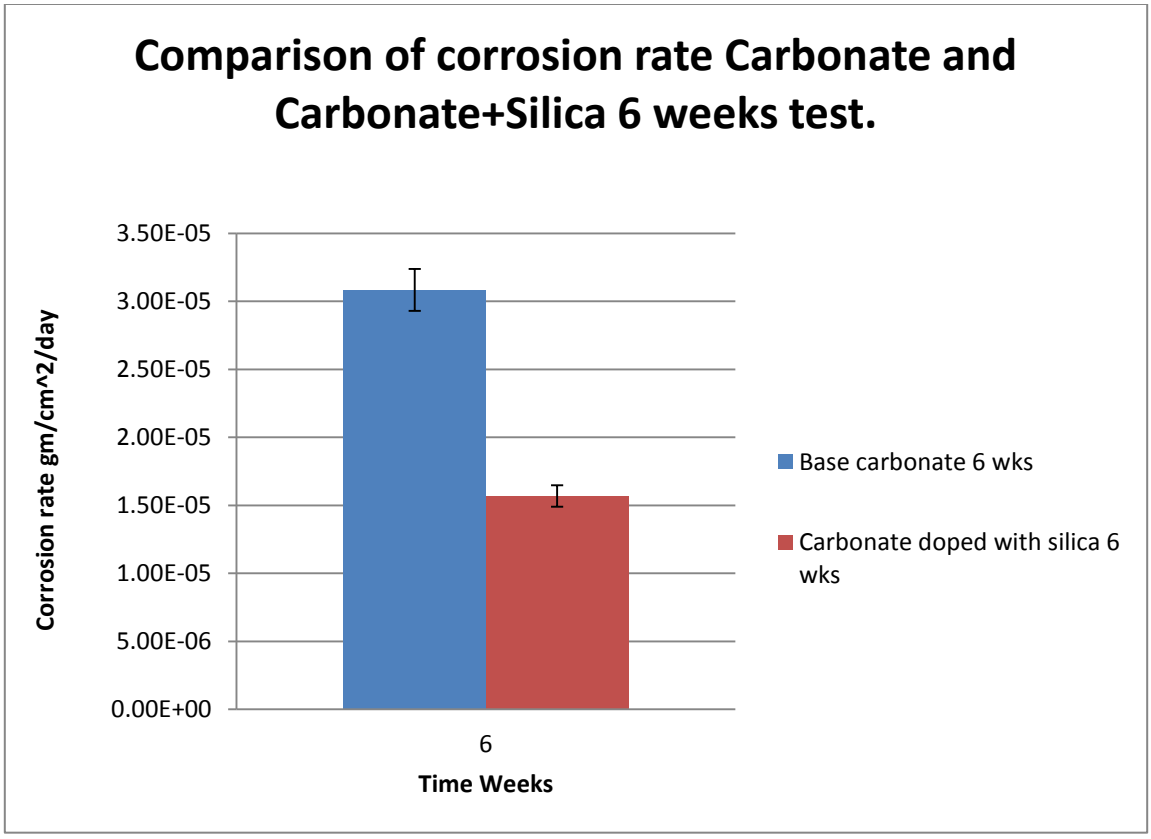

Figure 11: Instantaneous Corrosion rate Comparison between Carbonate and Carbonate Doped with Silica (6 weeks).

4.1.2 Comparison of Total Corrosion between Carbonate and Carbonate Doped with Silica

Figure 12 was constructed by plotting the average total mass loss per unit area against time. The bars indicate the mass loss per unit area at each time. Thus, the mass loss data of the steel coupons from the 2 week test normalized per unit area gives the total corrosion at 2 weeks. A similar statement holds for 4 and 6 weeks. This graph represents the corrosion characteristics of steel by molten plain and doped carbonate salts. This is compared with the theory where I expected a parabolic behavior. Both the carbonates

and carbonates doped with silica deviated from the parabolic behavior but exhibited the same behavior.

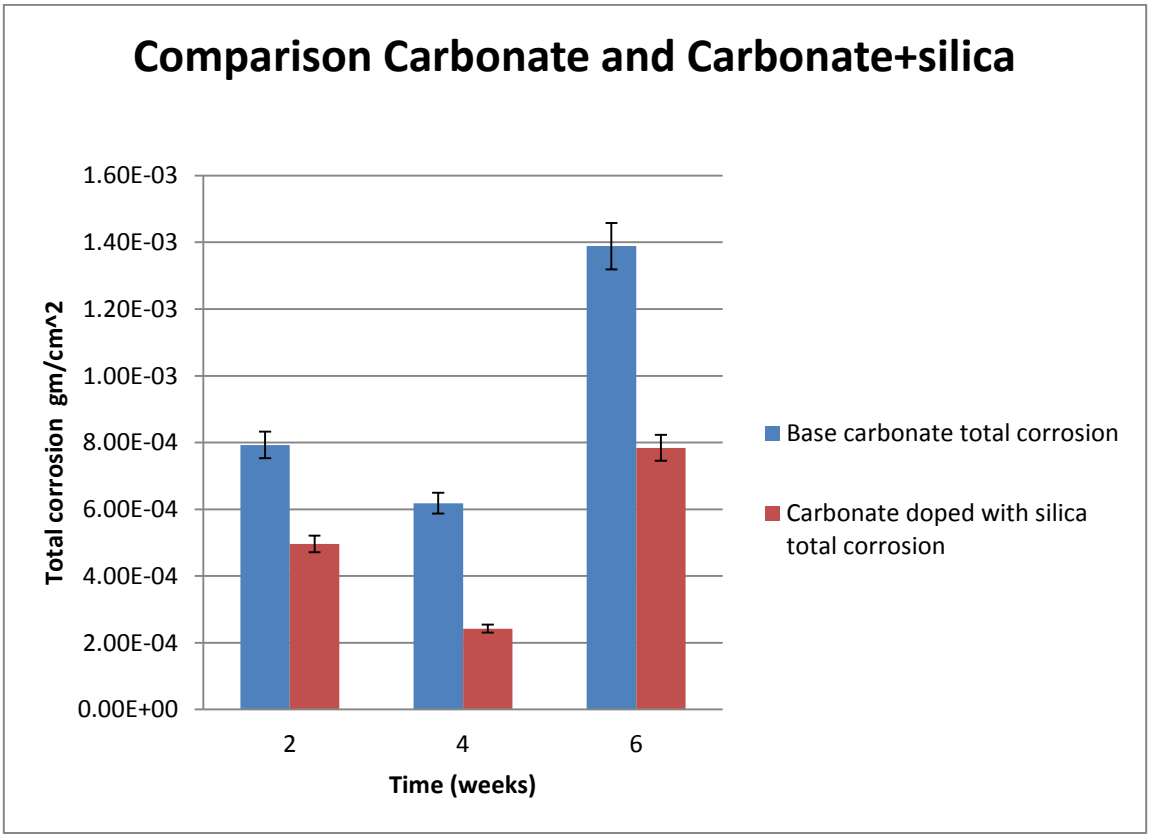

Figure 12: Total Mass Loss Comparison between Carbonate and Carbonate Doped with Silica.

4.2 Average Rate of Corrosion over all Exposure Times

The average rate of corrosion is determined to gauge the usability of the steel for CSP applications. By comparing the average rate and the predefined metric as per the Table 1 given in Cabeza et.al this thesis hopes to give qualitative recommendations on its applicability for CSP applications. The term average indicates average of average of

instantaneous corrosion rates over different exposure times. The Tables 3 and 4 below depicts the average corrosion rate by carbonate and carbonate doped with silica over all exposure times respectively.

Table 3: Average Corrosion Rate of Steel SS304 by Carbonate Eutectic at Different Timeframes.

Salt	Time (days)	Corrosion rate ($mg/cm^2/year$)
Carbonate	14	20.388
Carbonate	28	7.949
Carbonate	42	11.107

The average corrosion rate is 13.148

The corrosion rate due to carbonate doped with silica nanoparticles 1% by weight is depicted in Table 4.

Table 4: Average Corrosion Rate of Steel SS304 by Carbonate Doped with 1% Silica by Weight at Different Timeframes.

Salt	Time (days)	Corrosion rate ($mg/cm^2/year$)
Carbonate + silica	14	12.751
Carbonate + silica	28	3.24
Carbonate + silica	42	5.646

The average corrosion rate is 7.212

4.3 The Relative Percentage Decrease in Corrosion Due to Doping of Silica with Respect to Base Carbonate

Figure 13 was created by dividing the difference in corrosion between the base carbonate and the corrosion due to doping and dividing it (difference) by the corrosion due to base carbonate expressed in percentage. This Figure serves as a visual aid to perceive the effect of silica nanoparticles on corrosion.

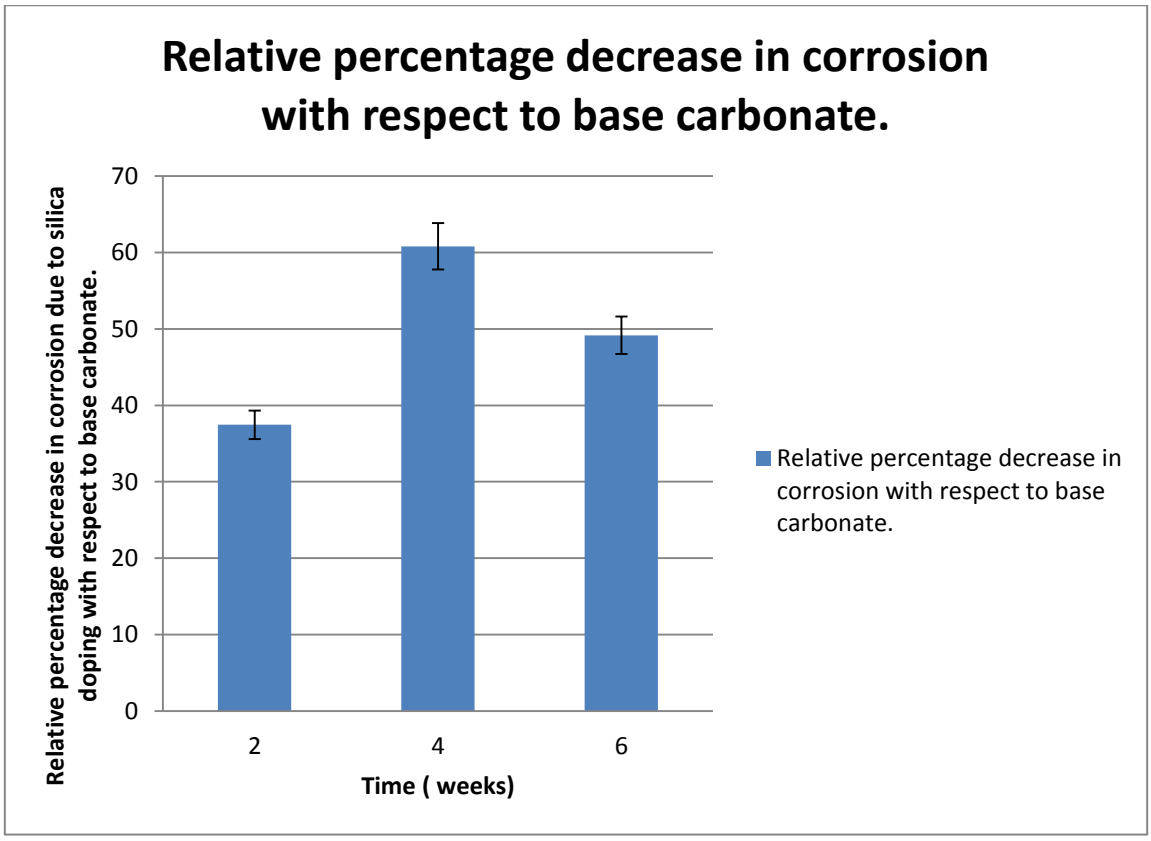

Figure 13: Relative Percentage Decrease in Corrosion Due to Doping of Silica.

4.4 Statistical Analysis

The results of this corrosion experiment showed an enhancement in the anticorrosive properties of molten carbonate by silica nanoparticles. These results must be statistically significant to make any claim valid in the discussions. This statistical analysis established the confidence level of the observations. A 2 tailed T test was performed to determine if the results are statistically significant. In this experiment the degrees of freedom were 4. This is arrived by determining the samples and subtracting 1 from each group. Since I am comparing 2 groups, with each group having 3 data points, the degree of freedom evaluates to 4 (2X3-2).

The confidence level was established as follows. I chose the confidence level of 95 %. The critical t-value for this confidence level and DoF is 2.1318. The Table 5 is the ‘t’ test result Table.

Table 5: 'T' Test Results Table for the Rate of Corrosion of Carbonates and Carbonates Doped with Silica for the Three Times.

T Test 95% confidence level	**Difference in Mean**	**(Var1/n1+var2/n2) 'J'**	**Sqrt(J)**	**t value (Mean/J)**	**Pass/Fail**
carbonate +silica 2 weeks	0.000021	5.44E-10	7.37E-06	2.875	**Pass**
Carbonate + silica 4 weeks	0.000013	3.38E-11	5.82E-06	2.3071	**Pass**
Carbonate + silica 6 weeks	0.000015	2.73E-11	5.23E-06	2.8988	**Pass**

5. DISCUSSION

First, the confounding effects are discussed. Then the results are discussed.

The experimental procedures adopted, though standardized may have been confounded due to-

a. The use of distilled water to remove the coupon from the ‘sample bomb’
b. The use of hydrochloric acid to descale the coupons.

I suspect the above two points could have confounded effects on the results because both the factors have a high possibility of inducing corrosion themselves. When such effects are not clearly quantified and isolated from my experiments, I could expect my results to be confounded. However, one way to argue that such confounding effects could be ignored is by saying that since all samples were subjected to the same process. The confounding effects could be eliminated by just focusing on the shift of the mean (corrosion rate) due to doping of silica. Nevertheless, it is important to make the reader aware of any possible confounding effects.

5.1 Possible Confounding Effects

In statistics, a confounding variable (also confounding factor, lurking variable) is an extraneous variable in a statistical model that correlates (positively or negatively) with both the dependent variable and the independent variable. In lay man’s terms, it can be described as an unforeseen and unaccounted-for variable that jeopardizes reliability and validity of an experiment's outcome.

This section discusses possible confounding effects from:

a. The use of distilled water to remove the coupon from the ‘sample bomb’
b. The use of hydrochloric acid to descale the coupons.

The use of distilled water: While removing the steel coupon from the sample bomb, it was sometimes necessary to use distilled water to free the steel coupon from the solidified melt. The time of such an exposure was approximately 2 days at maximum. This process may have confounded the experiment due to the effects of corrosion of the steel coupon by saturated salt water. Possible reasons for ignoring this confounding effect are:

1) The solution is not saturated and concentrated enough to cause enough corrosion.
2) The distilled water was replaced at least 3-4 times during that duration further reducing any possibility of saturation.

Though the above justification may be possible and applicable, the experiment results may have been confounded due to this adopted experimental process. The following change in the above mentioned process could overcome the confounding effects

i. Heat the sample bomb with the coupon inside to melt the salt. A frame could be built which would support open inverted sample bombs. When the salt melts, it would release the steel coupon. Care must be taken to contain nano-particles. This was one of the reasons to adopt the distilled water technique which would allow the removing of steel coupons in a safer manner.

ii. Use of a completely different design. Perhaps a sample bomb of glass could be constructed. This would allow the glass sample bomb to be shattered inside a glove box and allow safe removal of the steel coupon.

The use of hydrochloric acid for descaling: The problem with hydrochloric acid is that it is very corrosive and it corrodes steel. This agent was used to descale the oxide layers formed to measure the mass loss. The exposure time was a minute and the quantity of HCl used was 25 ml for descaling 3 samples. The concentration of the HCl was 30%. The confounding effect brought about by using HCl is that, given its corrosive nature, one cannot clearly ascertain if the mass loss that was measured was due to the testing corroding environment or due to the HCl acid. This is an important cause of confounding effect and must be considered while interpreting results. However, I justified the use because

1) The papers by Bradshaw et (9). Al and Cabeza et al (13) follow a similar process.
2) Other descaling methods like mechanical cleaning, in my opinion have more confounding effects. Mechanical descaling involves abrasive techniques. Now, abrasive descaling methodologies are more subjective and vary from user to user and thus confound the experiment even more.

However, I understand that this could be a significant cause of concern if the volume of HCl changes or the concentration changes. Corrosion is extremely environment dependent and as such my readings could have been biased. As such the results that follow must be interpreted with this effect in mind.

Remedy and Redesign of future experiments: Based on the literature review I find that for determining corrosion rate using mass loss, descaling is important and unavoidable. Any descaling process is questionable. Descaling is a macroscopic process and involves removal of just the oxides layers formed. Now, “removing just the oxide layers” is a very subjective and a questionable process. There is no one correct way of doing it. However processes can be standardized and ASTM has a standardized procedure. The ASTM procedure also uses HCl for descaling. However, the procedure I followed is a derived version of the ASTM G4-84 procedure. The only remedy is to use the standardized ASTM procedure for evaluation which is G4-84.

Final remarks: Based on the identified confounding effects of my experimental procedures, I would like to comment that all results, findings and conclusion must be viewed and interpreted with these stated effects in mind.

5.2 Discussion of Results

While discussing the results, first the corrosion rate is discussed and the possible reasons for decrease in corrosion due to silica are explained. Second the total corrosion is explained and compared with the expected corrosion characteristics and possible reasons for deviations are explained. Finally average corrosion rate is discussed as regards to the usability of steel in silica doped and without doped environment. The results above are discussed with respect to theory. Possible reasons for deviation from theory are discussed.

5.2.1 Corrosion Rate

The corrosion rate due to doping of silica nanoparticles decreased in all cases. My initial hypothesis was that, the corrosion rate of steel by molten carbonate salts would decrease by doping the carbonate salts with silica nanoparticles. The results agree with this hypothesis and show that corrosion rate has decreased in all cases. Silica nanoparticles may have formed a complex at the walls. These complexes would be very stable and must have formed very quickly at the initial exposure. This formation of complex could be acting as a passivating layer and prevent further corrosion. One way to confirm this explanation is by doing X-ray diffraction studies and then analyzing the complex. The nature of the complex should then hold the answer for this reduction in corrosion.

Another possibility is that silica nanoparticles could have migrated to the walls forming a barrier between the corroding environment and steel coupon. This can be confirmed and validated by studying the variation in concentration of nanoparticles in molten carbonate salts and focusing on the migration of nanoparticles towards wall, if any.

5.2.2 Total Corrosion

Figure 10 shows the total corrosion of carbonate and carbonate doped with silica nanoparticles. As can be seen from the figure, the total corrosion because of carbonate and carbonate doped with silica show a decrease in the total corrosion at 4 weeks (in comparison to 2 weeks) counter to the expected parabolic behavior. However, at 6 weeks, the total corrosion does show a marked increase. This observation (observed at 4 weeks) cannot be dismissed because of the high confidence level associated with these readings. This result suggests that further study must be done to identify the cause for

this decrease. One possible explanation for this decrease could be the formation of insoluble oxides which do not dissolve while descaling thereby creating a lower differential mass loss. Here the term solubility refers to the ease with which hydrochloric acid dissolves the oxides. X-ray diffraction studies of such oxides could offer insights on the composition and stability of such oxides. To further clarify, at 2 weeks the oxide layers formed could all or mostly have been soluble while at 4 weeks most of the oxides formed could have been insoluble and at 6 weeks further exposure (relative to 4 weeks) could have formed more soluble oxides (in addition to the insoluble oxides). This could explain the observed behavior. All steel coupons were descaled immediately after the respective test. This explanation needs to be further investigated and confirmed.

5.2.3 Average Corrosion Rate

The operability of steel under tested conditions has improved. On comparing the average corrosion rate from Table 3 and Table 4 with those mentioned in Table 1, I find that the recommendation for usage “Caution recommended, based on the specific application” with doping has improved to “Recommended for long term service.”

6. FINDINGS

The results were in accordance with initial hypothesis. The confidence in any finding is substantiated by the results in the statistical analysis. As per the hypothesis, I expected a decrease in the rate of corrosion due to adding silica nanoparticles. The rate of corrosion of steel by carbonate eutectics doped with silica nanoparticles was roughly half that of the rate of corrosion by the base carbonate for all time periods tested. Comparing the average rate of corrosion with and without doping, the recommendation for use without doping is “Caution recommended, based on the specific application” and with doping improves to “Recommended for long term service.”

7. CONCLUSION

I conclude that adding silica nanoparticles to the carbonate TES material will reduce the corrosion of SS304 under concentrated solar power plant conditions.

REFERENCES

1. National Energy Education Development Project 2008,"Solar at a glance," http://www.Need.org[Online]

2. Suegama, P.H. 2008 ″Corrosion behavior of carbon steel protected with single and bi-layer of silane films filled with silica nanoparticles," Surface & Coatings Technology **202,** pp.2850-2858.

3. Choi S.U.S. and Eastman J. A., November 1995, "Enhancing thermal conductivity of fluids with nanoparticles," Energy Technology Division and Materials Science Division, Argonne National Laboratory, Argonne IL

4. "Molten Salt Solar Energy Thermal Storage and Concentrated Solar Power (CSP) Market Shares, Strategies, and Forecasts, Worldwide, 2010 to 2016, " Market Research News, May 9 2011.

5. National Renewable Energy Laboratory September 2009**,** "Parabolic trough thermal energy storage technology". http://www.nrel.gov/csp/troughnet/thermal_energy_storage.html. [Online]

6. Behunek, I., February 2010, "Properties of inorganic PCM," Department of Electrical Power Engineering, Fakulta elektrotechniky a komunikačních technologií (FEEC).

7. Betts, M**.** 2011,"The effects of nanoparticle augmentation of nitrate thermal storage materials for use in concentrating solar power plants," M.S. thesis Texas A&M University College Station, TX.

8. S.D Cramer and B.S Covino,Jr(Eds.), ″Corrosion:Fundamentals, Testing and Protection ASM International"**.** Vol. 13 A**.**

9. Goods, S.H. and Bradshaw, R.W, 2004, "Corrosion of stainless steels and carbon steel by molten mixtures of commercial nitrate salts, "Journal of Materials Engineering and Performance, **13**(1), pp. 78-87.

10. Sadahiro T, Shinya N, Tadao W, 2006, "Correlation of grain boundary connectivity with grain boundary character distribution in austenitic stainless steel," Acta Materialia **54** 3617–3626, pp. 54.

11. Tomashov, N D**.** 1967, *Theory of Corrosion and Protection of Metals: The Science of Corrosion*. The Macmillan Company, New York.

12. Scott, L.R., Pile L. D. , Butt, P. D, 1998." Materials Corrosion and Mitigation Strategies for APT". Materials Corrosion & Environmental Effects Lab: Los Alamos National Laboratory, Los Alomos, NM..

13. Cabeza, L.F., Badia, F., Illa J., Roca, J.**,** Illa, J., Mehling, H., Heibler, S., Zeigler, F., 2001, "Immersion corrosion tests on metal-salt hydrate pairs used for latent heat storage in the 32 to 36^0 C temperature range," Material and Corrosion, **52**(2)**,** pp.140-146**.**

14. Tzvetkoff, T.Z., Girginov, A, Bojinov, M**.** 1995 "Review Corrosion of nickel, iron, cobalt and their alloys in molten salt electrolytes". , Journal of Material Science, **30**, pp. 5561-5575.

VITA

Name:	Ashwin Padmanaban Iyer
Address:	Texas A&M University
	Department of Mechanical Engineering
	3123 TAMU
	College Station, TX 77843-3123
	c/o Thomas Lalk or Michael Schuller
Email Address:	Ashwin.padmanaban@gmail.com
Education:	B.E. Mechanical Engineering, Visvesvaraya Technological University., June 2006
	M.S. Mechanical Engineering, Texas A&M University, May 2011